A smart self-balancing biosystem with reversible competitive adsorption of in-situ anion exchange resin for whole-cell catalysis preparation of lignocellulosic xylonic acid

Yang Lv [a, b, c], Shaonuo Zhou [a, b, c], Xiaolei Zhang[d] and Yong Xu* [a, b, c]

[a] *Jiangsu Co-Innovation Center of Efficient Processing and Utilization of Forest Resources, College of Chemical Engineering, Nanjing Forestry University, Nanjing 210037, People's Republic of China*

[b] *Jiangsu Province Key Laboratory of Green Biomass-based Fuels and Chemicals, Nanjing 210037, People's Republic of China*

[c] *Key Laboratory of Forestry Genetics & Biotechnology (Nanjing Forestry University), Ministry of Education, Nanjing 210037, People's Republic of China*

[d] *Department of Chemical and Process Engineering, University of Strathclyde, Glasgow, UK G1 1XJ*

* Corresponding author at: College of Chemical Engineering, Nanjing Forestry University. No. 159 Longpan Road, Nanjing 210037. People's Republic of China.

mail address: xuyong@njfu.edu.cn (Y. X.)

Tel: +86 025 85427587

Fax: +86 025 85427587

This is a peer-reviewed, accepted author manuscript of the following article: Lv, Y., Zhou, S., Zhang, X., & Xu, Y. (2022). A smart self-balancing biosystem with reversible competitive adsorption of in-situ anion exchange resin for whole-cell catalysis preparation of lignocellulosic xylonic acid. Bioresource Technology, 363, [127998]. https://doi.org/10.1016/j.biortech.2022.127998

Abstract:

Xylonic acid (XA) bioproduction via whole-cell catalysis of *Gluconobacter oxydans* is a promising strategy for xylose bioconversion, which is hindered by inhibitor formation during lignocellulosic hydrolysates. Therefore, it is important to develop a catalytic system that can directly utilize hydrolysate and efficiently produce XA. Determination of the dynamic adsorption characteristics of 335 anion exchange resin resulted in a unique and interesting reversible competitive adsorption between acetic acid-like bioinhibitor, fermentable sugar and XA. Xylose in crude lignocellulosic hydrolysates was completely oxidized to 52.52 g/L XA in unprecedented self-balancing biological system through reversible competition. The obtained results showed that in-situ resin adsorption significantly affected the direct utilization of crude lignocellulosic hydrolysate for XA bioproduction ($p \leq 0.05$). In addition, the resin adsorbed ca. 90% of XA during bioconversion. The study achieved a multiple functions and integrated system, "detoxification, neutralization and product separation" for one-pot bioreaction of lignocellulosic hydrolysate.

Key words: Xylonic acid, whole-cell catalysis, reversible competitive adsorption on resin, lignocellulosic bio-inhibitors, self-balancing biosystem.

46 # 1. Introduction

47 Xylonic acid (XA) is a water-soluble five-carbon organic acid with a wide range
48 of applications, including construction, aquaculture, biological control and chemical
49 industries (Chun et al., 2006; Deppenmeier et al., 2002; Znad et al., 2004), and is one
50 of the top 30 most valuable chemicals according to the U.S. Department of Energy
51 (Cao et al., 2013). In addition, XA is an important platform compound, a precursor of
52 3,4-dihydroxybutanal, 1,4-butanediol and 1,2,4-butantriol, and plays an indispensable
53 role in energetic materials synthesis and pharmaceutical production (Luo et al., 2020;
54 Zhou et al., 2016). It is reported that the whole cell catalytic preparation method of
55 XA production by *Gluconobacter oxydans* has high selectivity, cell reusability,
56 low-cost and high productivity, which is greatly advantageous compared to the
57 complicated chemical method and the expensive enzyme catalytic method (Chun et al.,
58 2006; Han et al., 2021; Jin et al., 2019).

59 It is known that the effective utilization of xylose can provide a higher profit to
60 the total entire biorefinery economy of lignocellulosic biomass. Additionally, there is
61 ca. 30% xylose content of fermentable carbohydrate compositions in lignocellulosic
62 materials, such as corncob and sugarcane bagasse (Jeffries et al., 2007; Li et al., 2018;
63 Menon & Rao, 2012). Therefore, the development of direct whole cell catalysis and
64 oxidation of acid hydrolysate to produce XA is of great practical significance for
65 xylose and lignocellulosic biomass biorefinery. However, various inevitable
66 degradation chemicals arise from lignocellulosic processing and results in complex
67 biotoxicity and bio-inhibition towards bacterial activity and cell catalysis performance.

68 These include types of HAc, such as small molecular acids, aldehydes, furans and so
69 on (Han et al., 2021; Horvath et al., 2001; Mhlongo et al., 2015). Even though resin
70 can achieve effective detoxification, it can promote considerable sugar loss by over 20%
71 (Lin & Juang, 2009; Schwartz & Lawoko, 2010). Therefore, it is necessary to develop
72 new methods for effective bioutilization of sugar adsorbed on resin.

73 During the whole cell catalytic oxidation of xylose to XA, pH value of the
74 system continuously decreases in relation to the corresponding acid formed, which
75 seriously hinders the catalytic activity of cells (Horvath et al., 2001; Hua et al., 2022).
76 Therefore, it is important to detect and monitor pH, and add an appropriate alkaline
77 neutralizer when required to maintain bioreaction niche stability. Studies have shown
78 that anion exchange resin can adsorb and neutralize automatically allowing the
79 production of XA as a basic agent (Liu et al., 2021a; Ortega et al., 2017).

80 Therefore, this study aims to construct a smart self-balancing biosystem for
81 lignocellulose-based xylonic acid production. The technical objectives of
82 "detoxification, neutralization and separation" were achieved simultaneously in a one
83 reaction tank via in-situ reversible competitive adsorption of anion exchange resin.
84 Furthermore, crude corncob hydrolysate was directly employed in XA bioproduction,
85 which has significance theoretical and practical applications in lignocellulosic
86 hydrolysate bioconversion.

87 2. Materials and methods

88 2.1 Lignocellulosic hydrolysate

89 Corncobs were harvested from Jiangsu Province in China. According to the

national Renewable Energy Laboratory protocol determination, corncob contains 34.4% cellulose, 30.5% hemicellulose and 18.6% lignin. Corncob was pulverized to 20-40 mesh size. Before pretreatment, all the sieved corncob were dried thoroughly in the sun and air until <8% moisture was obtained, then it was pretreated for 30 min at 150 ℃ with a solid-liquid ratio of 1:5 (w/v), 1% sulfuric acid (Gu et al., 2021). The resulting crude hydrolysate was called HA, and HB or HC which was twice concentrated or diluted from HA, respectively. The corresponding simulates of HA, HB and HC were called SA, SB and SC, respectively.

2.2 Pretreatment of resin

Weakly basic anion exchange resin 335 was prepared by reverse polymerization of epichlorohydrin and ethylene polyamine, bearing the following functional groups: $-NH_2$, =NH, and ≡N (Han et al., 2022). (Huazhen Company, East China University of Science and Technology)

The resin was soaked in ethanol solution of ca. twice the volume for 2-3 h. This process was repeated several times and then distilled water was added to the soaking solution without turbidity, followed by washing with distilled water until no ethanol remained. The eluent was shaken sequentially with 1 M NaOH, 1 M HCl and 1 M NaOH for 2 h, then cleaned with deionized water until neutral pH was obtained (Hua et al., 2018; Yue et al., 2018). Subsequently, the moisture content was measured by an infrared moisture meter to calculate the wet weight corresponding to the dry heavy ion exchange resin (Hua et al., 2018).

2.3 Adsorption of resin in simulated solution

2.3.1 Adsorption and desorption of resin in simulated solution

10% (w/v) resin was added to the three simulated solutions (SA, SB and SC), and the samples were placed in a shaker at 220 rpm and 30 ºC for 2 h to achieve adsorption equilibrium. The volume of the simulated liquid was 50 mL. The titer of various chemicals before and after adsorption was detected by HPAEC, and the adsorption ratio was calculated (Adsorption ratio=$\frac{Initial\ titer\ (g/L) - Titer\ after\ adsorption\ (g/L)}{Initial\ titer\ \ (g/L)}$). Subsequently, the resin was filtered and then placed in equal volumes of pure water, followed by shaking at 220 rpm, 30 ºC for 2 h. The titer of various chemicals before and after desorption was detected, and the desorption ratio was calculated (Desorption ratio=$\frac{Titer\ after\ desorption\ (g/L)}{Initial\ titer\ (g/L) - Titer\ after\ adsorption\ (g/L)}$).

2.3.2 Reversible competitive adsorption of various chemicals

Competitive adsorption of xylose and XA: 10% (w/v) resin was added to xylose simulation solution and xylose – XA mixture simulation solution, respectively. The adsorption equilibrium was reached by shaking at 220 rpm and 30 ℃ for 2 h. The titer of xylose and XA was detected, and the adsorption ratio was calculated.

Competitive adsorption of Hac and XA: 10% (w/v) resin was added to 10 g/L XA. After reaching the adsorption equilibrium, the resin was filtered out and then placed in 10 g/L HAc. In the control group, 10% resin was added to 10 g/L HAc, and the filtered resin was placed in 10 g/L XA after the adsorption equilibrium was reached.

2.4 Resin adsorption coupled with whole cell catalysis

134 Separate resin adsorption: SA was added to 20% resin and shaken at 200 rpm 30 ℃
135 for 2 h. The filtered SA was directly used for subsequent whole-cell catalysis (Han et
136 al., 2022).

137 In-situ resin adsorption: 20% resin was added at the beginning of whole cell
138 catalysis. The resin remained in the fermentation system throughout the experiment.

139 **2.5 Whole-cell catalysis of *Gluconobacter oxydans***

140 *G. oxydans* NL71 was derived from ATCC6821 and cultured for 18-24 h in
141 proliferation medium (100 g/L sorbitol, 10 g/L yeast extract) at 30 ℃ and 220 rpm
142 (Zhou et al., 2015). Proliferating cells were obtained by freeze-centrifugation at 7104
143 g for 5 min (Han et al., 2021). The synthetic medium contained 5.0 g/L yeast extract,
144 0.5 g/L $MgSO_4$, 2.0 g/L K_2HPO_4, 1.0 g/L KH_2PO_4, 5.0 g/L $(NH_4)_2SO_4$, and acidic
145 lignocellulosic hydrolysate (Liu et al., 2021b). Whole- cell catalysis was performed
146 by shaking at 200 rpm and 30 ℃ for 8-24 h in a 250 mL conical flask containing 50
147 mL medium. WCC was performed at a cell density of 5.0 g/L (oven dry weight).
148 Three independent biological replicates were conducted.

149 **2.6 Analytical methods**

150 The concentration of xylose and XA was determined by HPAEC (Thermo
151 ICS-5000) coupled with a CarboPac™ PA200 column and pulsed amperometric
152 detector. 100 mM NaOH solution was used as mobile phase at a flow rate of 0.3
153 mL/min (Han et al., 2021). The concentration of XA adsorbed by the resin was
154 measured by first rinsing the cells on the resin surface with deionized water and then
155 eluting with 5% hydrochloric acid (Han et al., 2022; Hua et al., 2018). HAc, levulinic

acid (LA), 5-hydroxymethyl-furfural (HMF) and furfural were analyzed via HPLC (Agilent 1200) equipped with Aminex Bio-Rad HPX-87H column and IR detector. 5.0 mM H_2SO_4 solution was used as mobile phase at 0.6 mL/min (Han et al., 2021; Han et al., 2022). Analysis of variance (ANOVA) was performed on the data using Microsoft Excel 2010 software. The data with statistical distribution is ($\overline{X}$±S). The significance level was α=0.05.

3. Results and discussion

3.1 Reversible competitive adsorption characteristics of various chemicals in stimulated solution

Anion exchange resin 335 contains weakly basic groups, such as primary amine group (-NH_2), secondary amine group (-NHR) or tertiary amine group (-NR_2), which usually dissociate -OH groups in water and act as a weak basic, especially under acidic conditions (Dharmapriya et al., 2022; Han et al., 2022). Therefore, this resin prefers to adsorb various generalized anion-like compounds in the lignocellulosic hydrolysate, including inhibitors of HAc, LA and so on (Cao et al., 2020; Huang et al., 2020), as well as xylose or newly generated XA. Firstly, the competitive adsorption characteristics of sugars and acids were investigated using 10% (w/v) resin 335 loading, in three gradient titers of stimulated solutions including SA, SB and SC (Table 1). The obtained results showed that the concentration of inhibitor compounds in SA and SC reduced by >60% after resin adsorption. Hence, the titer of key bio-inhibitor HAc was lower than the critical titer value that hinders bacterial fermentation(Zhou et al., 2019), and the detoxified solutions were directly utilized for

178 whole-cell catalysis and oxidation (Fig. 1). Although the resin adsorbed ca. 20% of
179 xylose-like sugars in 60.91 g/L sugar solution, 90% of the adsorbed sugars were
180 released from resin matrix into solution again in low sugar concentration
181 environments (Fig. 2). Therefore, the observed automatically reversible adsorption
182 and desorption, that depended on varying sugar titers, gave rise to the possibility to
183 explore in-situ resin adsorption coupled with whole-cell catalysis of fermented xylose
184 and lignocellulosic sugars.

185 Since XA is an organic acid with pK_a 3.39, the produced XA could also be
186 adsorbed on resin 335, allowing separate fermentation of the product and release the
187 product feedback inhibition on whole-cell catalysis. Hence, we investigated the
188 influence of XA production on the adsorption balance of xylose on the resin, which
189 could lead to competitive adsorption between xylose and XA. Based on the above
190 speculation, the competitive adsorption capacity of xylose, HAc and XA on the resin
191 was evaluated.

192 10% resin was added to xylose alone and xylose-XA mixture simulation
193 solutions, respectively. After adsorption equilibrium was reached, the xylose
194 concentration in the mixture was 2.12 g/L, and that in xylose alone was 1.39 g/L
195 (Table 2). Xylose-XA mixture simulation solution significantly affected the
196 adsorption ratio ($p \leq 0.05$). Hence, XA disturbed the adsorption balance of the xylose
197 and "squeezed" xylose out of the resin. In addition, most sugars can also "walk off "
198 the resin at low concentration (Fig.2). Thus, dual pressure could improve soluble
199 xylose for whole-cell catalysis and oxidation in the resin adsorption and detoxification

200 system.

201 10 g/L XA and 10 g/L HAc solution were also adsorbed by 10% resin,
202 respectively. After adsorption equilibrium was reached, residual XA and HAc in
203 solution were <10%, and HAc concentration was below the detection limit. To further
204 explore the competitive preference to HAc and XA on the studied resin, XA or HAc
205 adsorbed resin was poured in equal volumes of 10 g/L HAc and XA solution,
206 respectively. HAc could not elute XA adsorbed by resin, while XA could elute HAc
207 adsorbed by resin. 0.53 g/L HAc was eluted in the equalized solutions, indicating that
208 HAc was squeezed out by XA in the mixture (Table 3). This may be due the pKa
209 value of HAc being greater than that of XA, resulting in HAc bearing a weaker
210 binding force on the resin. This slightly stronger adsorption property provided an
211 interesting separation technology for XA harvest from xylose fermentation broth, as
212 well as another advantage of in-situ resin adsorption coupled with whole-cell catalysis,
213 especially under HAc-like bio-inhibitors pressure.

214 **3.2 Dynamic balance and coupling effects of in-situ resin adsorption combined**
215 **with whole-cell catalysis**

216 In terms of crude lignocellulosic hydrolysates components, a full-component
217 simulation was used to study the combination of in-situ resin adsorption with whole
218 cell catalysis. Pretreatment of lignocellulosic biomass produced a variety of
219 compounds that severely inhibited energy generation, enzyme activity and protein
220 synthesis in microbial central carbon metabolic pathways, which enhanced bacterial
221 cell survival and made fermentation impossible in the crude hydrolysates without

222 detoxification (Holscher & Gorisch, 2006).

223 The separated-resin and in-situ resin adsorption modes were compared. At the
224 preliminary stage, the fermentation rate of the simulant adsorbed by the separated
225 resin was fast. 51.71 g/L XA was obtained after 16 h at the initial productivity of 3.79
226 g/L/h, but the rate gradually decreased with the accumulation of sugar acid. In
227 contrast, the dynamic adsorption of in-situ resin adsorption mode maintained a
228 fermentation rate of up to 3.93 g/L/h after the first stage. Although XA was detected
229 in the medium during fermentation, 52.63 g/L XA was almost completely adsorbed by
230 the resin at the end of fermentation (Fig. 3).

231 Due to the beneficial cooperation of in-situ resin, the pH value of the whole-cell
232 catalysis system was stabilized by an automatic neutralization process. Furthermore,
233 the competitive adsorption and slow acetate release led to an efficiently gradual
234 bio-adaptation of bacterial cells for whole cell catalysis and oxidation. In conjugation
235 with oxidative conversion and metabolism of some inhibitors, the desired
236 comprehensive result of bio-toxicity reduction was achieved (Zhou et al., 2017).
237 Based on the dynamic equilibrium of resin adsorption, the dual effects of higher pK_a
238 and rising titer of XA competed and squeezed the resin-bonded xylose promoting
239 release and return to the fermentation medium(Chowdhury et al., 2011). The extruded
240 xylose was oxidated to XA and significantly improved the total product-yield of
241 whole-cell catalysis ($p \leq 0.05$). Furthermore, the priorly competitive adsorption was
242 selectively capture XA from the fermentation broth that provided an easy method for
243 both product separation and purification.

244 **3.3 Direct XA bio-preparation from crude corncob hydrolysate in the**
245 **self-balancing biosystem**

246 Considering the direct utilization of crude lignocellulosic hydrolysate,
247 hydrolysate A without any pretreatment was first tested (Lin & Juang, 2009). As
248 shown in Fig. 3, hydrolysate A was directly used for XA production by *G. oxydans*
249 with in-situ resin adsorption. At the early stage of fermentation (0-2 h), the inhibitor
250 titer gradually reduced and remained at a low level (<1 g/L) due to ion exchange
251 between the inhibitors and resin, which benefited *G. oxydans* to gradually adapt to the
252 inhibitory environment and perform its catalytic oxidation to xylose. Despite the more
253 complex competing anions from degrading fractions in crude lignocellulosic
254 hydrolysates, the free XA concentration in the fermentation solution remained
255 consistently low (<10 g/L), even when self-accumulating during whole-cell catalysis.
256 Therefore, XA maintained a stronger adsorption to the resin over the above
257 competitors. Resin adsorbed and harvested 90% of XA product from the crude
258 lignocellulosic fermentation broth containing 52.52 g/L of XA (Fig. 4). p-value was
259 0.12, indicating that there was no significant difference between biological replicates.
260 Hence, one could define the developed in-situ resin combined with whole-cell
261 catalysis as a smart self-balancing biosystem for XA bioproduction from crude
262 lignocellulosic xylose.

263 In this study the specific cell-catalysis efficiency (SCE) was proposed to
264 comparatively assess the total XA bioconversion performance of different whole-cell
265 catalysis modes by *G. oxydans* (see supplementary materials). SCE was determined as

0.46 g/L/h/g DCW using calcium hydroxide neutralization and precipitation of crude hydrolysate before whole-cell catalysis (Han et al., 2021). This value was improved to 0.50 g/L/h/g DCW after replacement with high-oxygen tension fermentation (Zhou et al., 2015). However, the self-balancing biosystem directly catalyzed crude corncob hydrolysate and increased SEC to 0.53 g/L/h/ g DCW without Ca-based detoxification, which was only slight lower than 0.58 g/L/h/ g DCW for the full-component analog solution. This fluctuation was probably related to the complexity of the various undetected components in crude corncob hydrolysate (Zhou et al., 2015; Zhou et al., 2017). Hence, the self-balancing system allowed the cells to ferment directly to crude lignocellulosic hydrolysate, and achieve enhanced cellular productivity.

4. Conclusion

Harnessing the advantageous properties of anion exchange resin 335 in-situ coupled with whole-cell catalysis, allowed for the development of a smart self-balancing biological system that resulted in "detoxification, neutralization and product separation" in a one-pot bioreaction and the realization of effective XA production directly from crude hydrolysate. The combinative process is important for the theoretical development and practical application of XA bioproduct production from lignocellulosic biomass, owing to its uniqueness, simplicity.

Conflicts of interest

There are no conflicts to declare.

Acknowledgement

Acknowledgements

The research was supported by the National Natural Science Foundation of China (32171730, 32211530071). The authors also would like to thank support from the Royal Society International Exchanges 2021 Cost Share grant IEC\NSFC\211370, EPSRC grant EP/R010986/1 and Leverhulme Trust Research Grant RPG-2017-254, UK.

Reference

Cao, R., Guo, J.M., Hua, X., Xu, Y. 2020. Investigation on decolorization kinetics and thermodynamics of lignocellulosic xylooligosaccharides by highly selective adsorption with Amberlite XAD-16N. *Food Chemistry*, **310**.

Cao, Y.J., Xian, M., Zou, H.B., Zhang, H.B. 2013. Metabolic Engineering of Escherichia coli for the Production of Xylonate. *Plos One*, **8**(7).

Chowdhury, Z.Z., Zain, S.M., Rashid, A.K. 2011. Equilibrium Isotherm Modeling, Kinetics and Thermodynamics Study for Removal of Lead from Waste Water. *E-Journal of Chemistry*, **8**(1), 333-339.

Chun, B.W., Dair, B., Macuch, P.J., Wiebe, D., Porteneuve, C., Jeknavorian, A. 2006. The development of cement and concrete additive. *Applied Biochemistry and Biotechnology*, **131**(1-3), 645-658.

Deppenmeier, U., Hoffmeister, M., Prust, C. 2002. Biochemistry and biotechnological applications of Gluconobacter strains. *Applied Microbiology and Biotechnology*, **60**(3), 233-242.

Dharmapriya, T.N., Shih, H.Y., Huang, P.J. 2022. Facile Synthesis of Hydrogel-Based Ion-Exchange Resins for Nitrite/Nitrate Removal and Studies of Adsorption

310 Behavior. *Polymers*, **14**(7).

311 Gu, Y.J., Guo, J.M., Nawaz, A., ul Haq, I., Zhou, X., Xu, Y. 2021. Comprehensive
312 investigation of multiples factors in sulfuric acid pretreatment on the
313 enzymatic hydrolysis of waste straw cellulose. *Bioresource Technology*, **340**.

314 Han, J., Hua, X., Zhou, X., Xu, B., Wang, H., Huang, G.H., Xu, Y. 2021. A
315 cost-practical cell-recycling process for xylonic acid bioproduction from
316 acidic lignocellulosic hydrolysate with whole-cell catalysis of Gluconobacter
317 oxydans. *Bioresource Technology*, **333**.

318 Han, J., Xu, B., Wang, H., Huang, G., Zhang, X., Xu, Y.J.B.t. 2022. Purification of
319 acidic lignocellulose hydrolysate using anion-exchange resin: Multicomponent
320 adsorption, kinetic and thermodynamic study. **351**, 126979.

321 Holscher, T., Gorisch, H. 2006. Knockout and overexpression of pyrroloquinoline
322 quinone biosynthetic genes in Gluconobacter oxydans 621H. *Journal of*
323 *Bacteriology*, **188**(21), 7668-7676.

324 Horvath, I.S., Taherzadeh, M.J., Niklasson, C., Liden, G. 2001. Effects of furfural on
325 anaerobic continuous cultivation of Saccharomyces cerevisiae. *Biotechnology*
326 *and Bioengineering*, **75**(5), 540-549.

327 Hua, X., Cao, R., Zhou, X., Xu, Y. 2018. Integrated process for scalable bioproduction
328 of glycolic acid from cell catalysis of ethylene glycol. *Bioresource Technology*,
329 **268**, 402-407.

330 Hua, X., Zhang, C.H., Han, J., Xu, Y. 2022. pH regulatory divergent point for the
331 selective bio-oxidation of primary diols during resting cell catalysis.

Biotechnology for Biofuels and Bioproducts, **15**(1).

Huang, C.X., Zheng, Y.Y., Lin, W.Q., Shi, Y.X., Huang, G.H., Yong, Q. 2020. Removal of fermentation inhibitors from pre-hydrolysis liquor using polystyrene divinylbenzene resin. *Biotechnology for Biofuels*, **13**(1).

Jeffries, T.W., Grigoriev, I.V., Grimwood, J., Laplaza, J.M., Aerts, A., Salamov, A., Schmutz, J., Lindquist, E., Dehal, P., Shapiro, H., Jin, Y.S., Passoth, V., Richardson, P.M. 2007. Genome sequence of the lignocellulose-bioconverting and xylose-fermenting yeast Pichia stipitis. *Nature Biotechnology*, **25**(3), 319-326.

Jin, C., Hou, W.L., Yao, R.M., Zhou, P.P., Zhang, H.S., Bao, J. 2019. Adaptive evolution of Gluconobacter oxydans accelerates the conversion rate of non-glucose sugars derived from lignocellulose biomass. *Bioresource Technology*, **289**.

Li, C., Gai, Z.C., Wang, K., Jin, L.P. 2018. Engineering Bacillus licheniformis as a thermophilic platform for the production of L-lactic acid from lignocellulose-derived sugars (Retraction of Vol 10, art no 235, 2017). *Biotechnology for Biofuels*, **11**.

Lin, S.H., Juang, R.S. 2009. Adsorption of phenol and its derivatives from water using synthetic resins and low-cost natural adsorbents: A review. *Journal of Environmental Management*, **90**(3), 1336-1349.

Liu, J.C., Zhang, Y.B., Miao, Y., Yang, Y., Li, P. 2021a. Alkaline Resins Enhancing Li+/H+ Ion Exchange for Lithium Recovery from Brines Using Granular

354 Titanium-Type Lithium Ion-Sieves. *Industrial & Engineering Chemistry*
355 *Research*, **60**(45), 16457-16468.
356 Liu, X.L., Cao, R., Nawaz, A., ul Haq, I., Zhou, X., Xu, Y. 2021b. Smart removal of
357 monosaccharide contaminants in xylo-oligosaccharide slurry using
358 sandwich-integration bioprocess of whole-cell catalysis combined with
359 electrodialysis separation. *Renewable Energy*, **168**, 1149-1156.
360 Luo, J., Huang, K.X., Zhou, X., Xu, Y. 2020. Preparation of highly flexible and
361 sustainable lignin-rich nanocellulose film containing xylonic acid (XA), and
362 its application as an antibacterial agent. *International Journal of Biological*
363 *Macromolecules*, **163**, 1565-1571.
364 Menon, V., Rao, M. 2012. Trends in bioconversion of lignocellulose: Biofuels,
365 platform chemicals & biorefinery concept. *Progress in Energy and*
366 *Combustion Science*, **38**(4), 522-550.
367 Mhlongo, S.I., den Haan, R., Viljoen-Bloom, M., van Zyl, W.H. 2015. Lignocellulosic
368 hydrolysate inhibitors selectively inhibit/deactivate cellulase performance.
369 *Enzyme and Microbial Technology*, **81**, 16-22.
370 Ortega, A., Oliva, I., Contreras, K.E., Gonzalez, I., Cruz-Diaz, M.R., Rivero, E.P.
371 2017. Arsenic removal from water by hybrid electro-regenerated anion
372 exchange resin/electrodialysis process. *Separation and Purification*
373 *Technology*, **184**, 319-326.
374 Schwartz, T.J., Lawoko, M. 2010. Removal of Acid-Soluble Lignin from Biomass
375 Extracts Using Amberlite Xad-4 Resin. *Bioresources*, **5**(4), 2337-2347.

Yue, S.J., Bilal, M., Song, C., Guo, S.Q., Li, S., Huang, P., Hu, H.B., Wang, W., Zhang, X.H. 2018. Development of an efficient method for separation and purification of brans2,3-dihydro-3-hydroxyanthranilic acid from Pseudomonas chlororaphis GP72 fermentation broth. *Separation and Purification Technology*, **202**, 144-148.

Zhou, P.P., Yao, R.M., Zhang, H.S., Bao, J. 2019. Unique glucose oxidation catalysis of Gluconobacter oxydans constitutes an efficient cellulosic gluconic acid fermentation free of inhibitory compounds disturbance. *Biotechnology and Bioengineering*, **116**(9), 2191-2199.

Zhou, X., Lu, S.S., Xu, Y., Mo, Y.X., Yu, S.Y. 2015. Improving the performance of cell biocatalysis and the productivity of xylonic acid using a compressed oxygen supply. *Biochemical Engineering Journal*, **93**, 196-199.

Zhou, X., Xu, Y., Yu, S.Y. 2016. Simultaneous Bioconversion of Xylose and Glycerol to Xylonic Acid and 1,3-Dihydroxyacetone from the Mixture of Pre-Hydrolysates and Ethanol-Fermented Waste Liquid by Gluconobacter oxydans. *Applied Biochemistry and Biotechnology*, **178**(1), 1-8.

Zhou, X.L., Zhou, X., Xu, Y., Chen, R.R. 2017. Gluconobacter oxydans (ATCC 621H) catalyzed oxidation of furfural for detoxification of furfural and bioproduction of furoic acid. *Journal of Chemical Technology and Biotechnology*, **92**(6), 1285-1289.

Znad, H., Markos, J., Bales, V. 2004. Production of gluconic acid from glucose by Aspergillus niger: growth and non-growth conditions. *Process Biochemistry*,

39(11), 1341-1345.

401 **Figure captions**

402 **Fig. 1** Adsorption and desorption of three simulated solutions on resin ($p>0.05$).
403 (A) and (C) represent the adsorption of sugars and inhibitors, respectively. (B) and
404 (D) represent the desorption of the corresponding adsorbed resin at low
405 concentration.

406 **Fig. 2** Schematic diagram of reversible competitive adsorption of various
407 components on resin.

408 **Fig. 3** Comparison of fermentation curves by using two resin adsorption modes in
409 stimulated solution ($p>0.05$).
410 (A) The separate resin adsorption (B) The in-situ resin adsorption

411 **Fig. 4** XA bioproduction from the crude lignocellulosic hydrolysate by in-situ
412 resin adsorption coupled with whole-cell catalysis ($p>0.05$).
413

414 **Table 1** Main component titers in three crude corncob hydrolysates (g/L)

Stimulants	GLU	XYL	Ara	HAc	LA	HMF	Furfural
HA	8.63±0.22	60.91±0.24	7.12±0.03	5.37±0.02	0.71±0.02	0.07±0.01	0.64±0.02
HB	17.80±0.12*	127.23±0.31*	14.77±0.07*	11.24±0.21*	1.59±0.13*	0.34±0.02*	1.45±0.14*
HC	3.76±0.04*	26.89±0.11*	3.07±0.01*	2.23±0.05*	0.29±0.02*	0*	0.27±0.03*

415 Note: There were significant differences among HA, HB and HC, *P<0.05.

416

417 **Table 2** The In-situ adsorption of stimulated solution by resin

Simulants	XYL		XYL+XA	
	XYL (g/L)	XA (g/L)	XYL (g/L)	XA (g/L)
Initial	2.56±0.05	0	2.57±0.03	26.21±0.24
Equilibrium	1.39±0.02	0	2.12±0.02	3.17±0.04
Adsorption ratio	45.7%	0	17.5% *	87.9% *

418 Note: Xylose – XA mixture simulation solution has a significant effect on the adsorption ratio,

419 $^{*}P<0.05$.

420

421 **Table 3** Comparison of adsorption priority of HAc and XA on resin (g/L)

Simulants	HAc elutes XA on resin		XA elutes HAc on resin	
	XA	HAc	XA	HAc
Acidic component	9.87±0.23	0	0	9.79±0.24
After resin adsorption	1.02±0.21	0	0	0
After Hac/XA elutes the used resin	0	0.22±0.03	1.53±0.04	0.53±0.02

422

423

Fig. 1

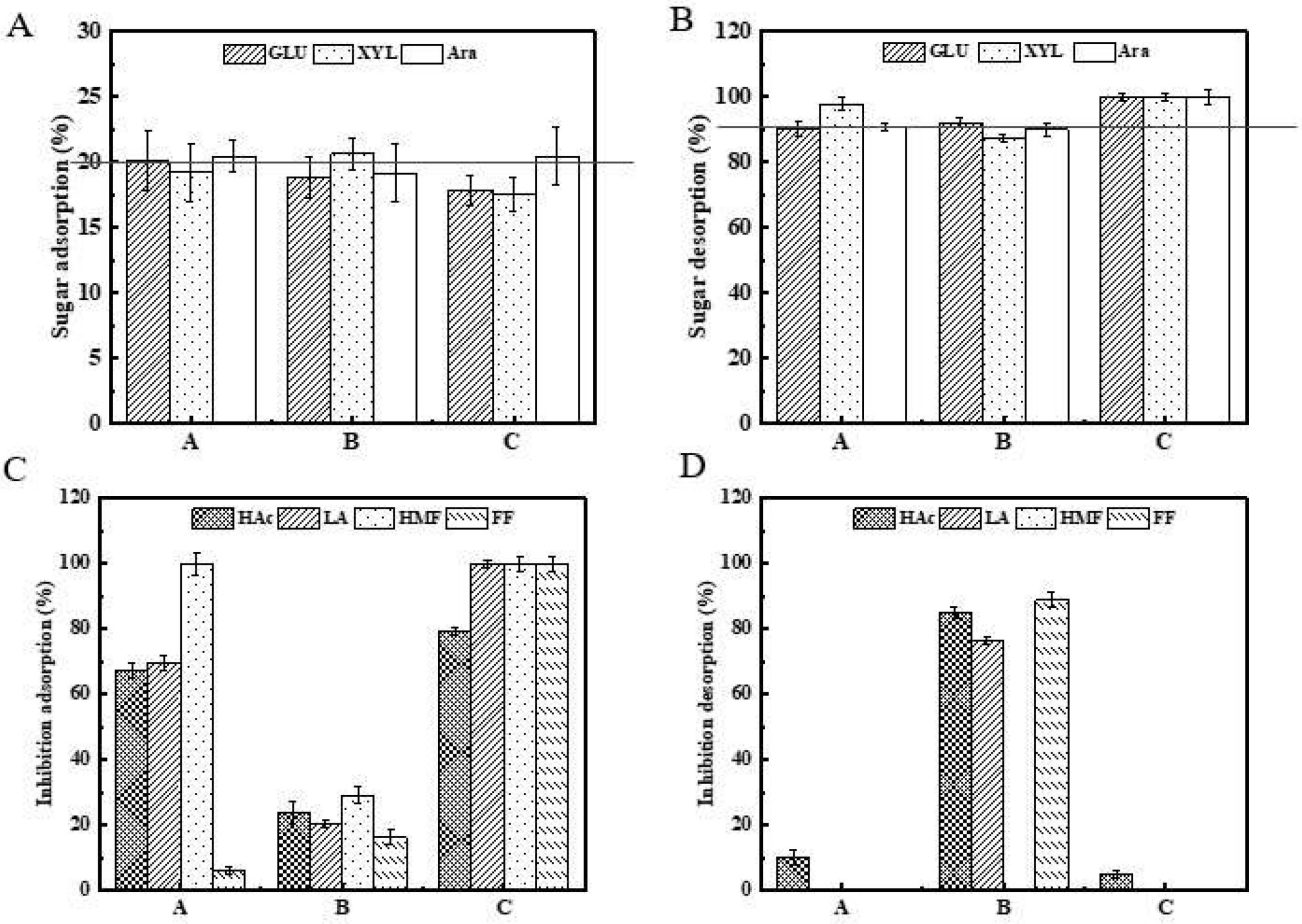
A
GLU
XYL
Ara
Sugar adsorption (%)
B
Sugar desorption (%)
C
HAc
LA
HMF
FF
Inhibition adsorption (%)
D
Inhibition desorption (%)
A
B
C

Fig. 2

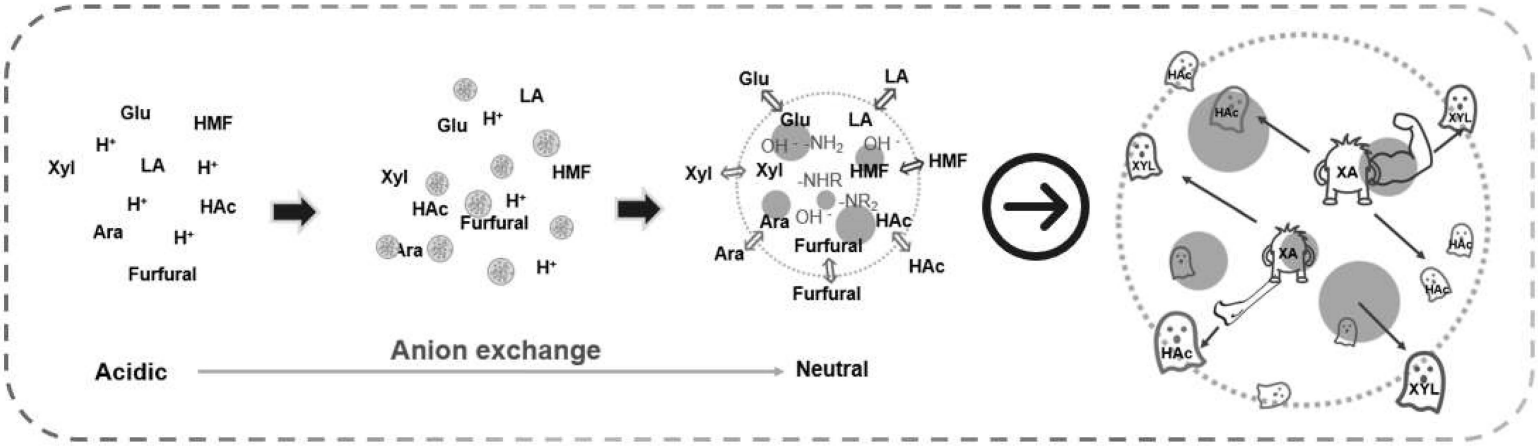
Glu
HMF
H+
Xyl
LA
H+
H+
HAc
Ara
H+
Furfural
LA
Glu
H+
Xyl
HMF
HAc
H+
Furfural
Ara
H+
Glu
LA
Glu
LA
OH-
-NH2
OH-
Xyl
Xyl
HMF
HMF
-NHR
-NR2
Ara
OH-
HAc
Furfural
Ara
HAc
Furfural
HAc
XYL
XA
XA
HAc
HAc
XYL
HAc
XYL
Acidic
Anion exchange
Neutral

Fig. 3

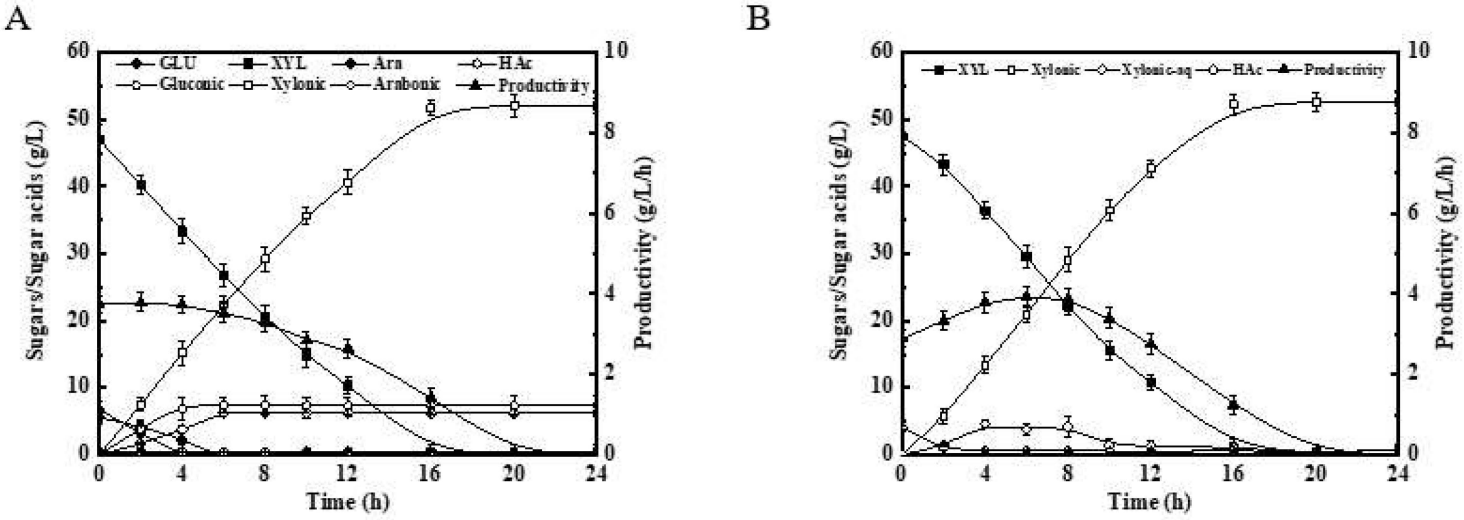
A
GLU
XYL
Ara
HAc
Gluconic
Xylonic
Arabonic
Productivity
Sugars/Sugar acids (g/L)
Productivity (g/L/h)
Time (h)
B
XYL
Xylonic
Xylonic-aq
HAc
Productivity
Sugars/Sugar acids (g/L)
Productivity (g/L/h)
Time (h)

434 **Fig. 4**

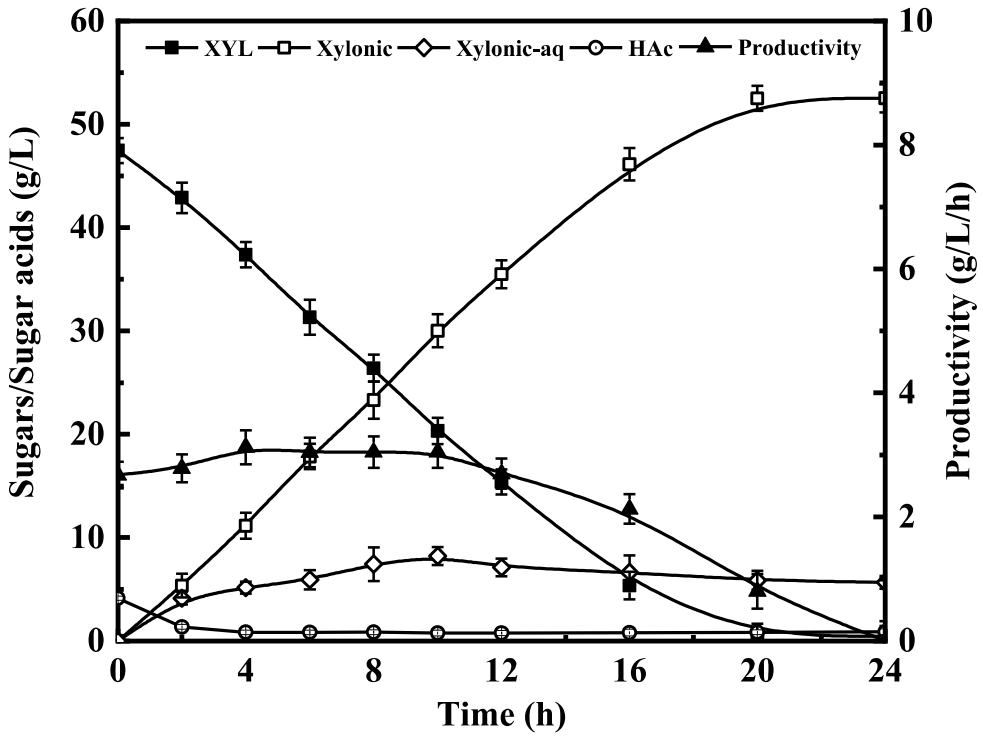

435

436